water

MDPI

Article

Isotopic Composition of Precipitation and Its Role in Forest Hydrology Under Climate Change: Insights from Slovenian Lowland Forests

Katja Koren Pepelnik [1,2,*], Mitja Janža [1], Matjaž Čater [3,4], Barbara Čenčur Curk [5] and Polona Vreča [6]

[1] Geological Survey of Slovenia, 1000 Ljubljana, Slovenia; mitja.janza@geo-zs.si
[2] Environmental Protection, University of Ljubljana, Kongresni trg 12, 1000 Ljubljana, Slovenia
[3] Slovenian Forestry Institute, Večna pot 2, 1000 Ljubljana, Slovenia; matjaz.cater@gozdis.si
[4] Faculty of Forestry and Wood Technology, Mendel University, Zemedelska 3, 61300 Brno, Czech Republic
[5] Department of Geology, Faculty of Natural Science and Technology, University of Ljubljana, Aškerčeva Cesta 12, 1000 Ljubljana, Slovenia; barbara.cencur@ntf.uni-lj.si
[6] Department of Environmental Sciences, Jožef Stefan Institute, Jamova 39, 1000 Ljubljana, Slovenia; polona.vreca@ijs.si
* Correspondence: katja.koren@geo-zs.si; Tel.: +386-1-280-9787

Abstract

Monitoring of stable isotopes in throughfall ($\delta^{18}O$, $\delta^{2}H$) and meteorological parameters is a valuable tool for researching forest hydrology, particularly during extreme events like droughts and floods. This study presents the first systematic analysis of air temperature and precipitation changes over the past 65 years in two Slovenian lowland forests: Murska šuma and Krakovski gozd, in combination with isotopic composition research of throughfall. The observed rising air temperatures and altered precipitation patterns are reflected in the isotopic composition of throughfall. Over the last 65 years, air temperature has increased by approximately 2.5 °C. Although total annual precipitation amounts have remained relatively stable, in the last 35 years there is a notable decrease in precipitation in growing season and an increase during the dormant season, influenced by air masses of Mediterranean origin. Extreme drought in 2022 and flood in 2023 are confirmed by the Standardized Precipitation Index and isotopic variations in throughfall due to fractionation processes. Annual variability appears as seasonal changes, with sine-curve amplitudes of 3.71‰ in Krakovski gozd and 3.61‰ in Murska šuma. Together with the Local Meteoric Water Lines, these patterns support estimates of groundwater mean residence time and the origin of water used by trees.

Keywords: stable isotopes; oxygen; hydrogen; climate change; hydrology forest; throughfall; Standardized Precipitation Index

Academic Editor: Cesar Andrade

Received: 9 February 2026
Revised: 15 March 2026
Accepted: 21 March 2026
Published: 23 March 2026

1. Introduction

Understanding forest hydrological processes is increasingly important due to the high mortality rates observed in many forest ecosystems [1,2]. This issue is often attributed to the lowering of the groundwater table and the resulting reduced accessibility of groundwater to trees, driven by anthropogenic pressures and climate change, changes in the amount and temporal distribution of precipitation recharge, and the increasing frequency of extreme events such as droughts and floods [3–5]. Forests profoundly influence local water balance and microclimate and play a key role in the global carbon cycle by storing carbon in

biomass and soil organic matter [6,7]. This carbon sequestration contributes to climate change mitigation by removing CO_2 from the atmosphere [8].

Within the forest, tree canopies regulate hydrological and energy fluxes [9]. Trees extract soil water within the reach of their roots and return a large portion of it to the atmosphere through transpiration [10,11], contributing to evaporative cooling and microclimate regulation [12–14]. Consequently, deforestation can disrupt this process, leading to increased air temperatures and altered water fluxes [15].

In the past decades, high mortality rates have been observed in groundwater-dependent ecosystems (GDEs) of several lowland oak forests in Slovenia [16,17], including the pilot areas of Murska šuma and Krakovski gozd, as well as in other parts of Europe between 1984 and 2016 [18]. These impacts were particularly pronounced in dry and warm regions, such as parts of the Iberian Peninsula and southeastern Europe, where oak species are dominant [19].

Drought is one of the main stressors affecting these ecosystems and can be classified as meteorological, agricultural, or hydrological [20]. Meteorological drought is linked to precipitation deficits and high temperatures, which reduce infiltration, runoff, and groundwater recharge [21]. The Standardized Precipitation Index (SPI) is widely used to quantify deviations from long-term precipitation averages and to detect drought conditions [22,23]. In Slovenia, drought has been declared a natural disaster seven times since 2000, with particularly severe events in 2003, 2012, 2013, 2017, and 2022 [22]. In contrast, extreme hydrological conditions occurred in August 2023, when northern and central parts of Slovenia experienced extreme rainfall and unusually wet summer conditions, including high soil moisture and precipitation with return periods estimated between 250 and 500 years [24].

Forest canopies intercept a significant proportion of precipitation, and the interception process depends on vegetation characteristics such as canopy structure, leaf area index, and tree morphology [25,26]. Some intercepted rainfall evaporates back into the atmosphere, while the rest reaches the forest floor as throughfall or stemflow [27]. Throughfall thus represents the portion of precipitation that reaches the soil after canopy interaction and contributes to soil moisture, subsurface flow, and groundwater recharge, depending on soil properties, antecedent conditions, and rainfall characteristics [25,28,29].

Stable isotopes of oxygen ($\delta^{18}O$) and hydrogen ($\delta^{2}H$) are powerful tools for investigating hydrological processes within forest ecosystems [30,31]. As precipitation passes through the canopy, interception evaporation and mixing processes alter the isotopic composition, often resulting in throughfall enriched in heavy isotopes compared to open precipitation [32]. Despite growing evidence of climate-related stress in groundwater-dependent forests, isotopic studies of precipitation–canopy interactions and throughfall dynamics remain relatively limited [33]. Tritium can provide additional information on water residence times in groundwater systems; however, it is not routinely used in plant water studies because a large amount of water is needed and the analysis costs are high. Therefore, to maintain methodological consistency across all investigated water matrices, tritium has been excluded.

In Slovenia, monitoring of the isotopic composition of precipitation has been conducted at meteorological and research stations since 1981 [34,35]. All these stations are in “open space”, whereas forest ecosystems, where precipitation dynamics differ, have not yet been studied. Reliable isotopic data for these processes in the case of Slovenian lowland forests, defined also as groundwater-dependent ecosystems, have only become available since systematic monthly sampling of a composite of throughfall in Murska šuma and Krakovski gozd began. Although the current record covers only several years, these data represent the first consistent isotope dataset for these groundwater-dependent forest systems. Combined with analyses of precipitation, groundwater, and xylem water, such

isotopic information provides valuable insights into groundwater mean transit times and the partitioning of water sources used by trees [36–38].

The newly established isotope dataset of throughfall from Murska šuma and Krakovski gozd therefore offers a unique opportunity to assess canopy-driven isotopic modifications of precipitation and to enhance understanding of water sources and hydrological processes governing groundwater-dependent forest ecosystems.

The study aims to (i) assess the long-term trends in temperature and precipitation amount in the Krakovski gozd and Murska šuma forests over the past 65 years and (ii) examine whether such changes or extreme weather events are detectable through variations in the isotopic composition of oxygen and hydrogen ($\delta^{18}O$ and $\delta^{2}H$) in throughfall; and (iii) characterize the isotopic composition and seasonal variability of local precipitation to define the baseline isotopic input to the hydrological system.

2. Materials and Methods

2.1. Pilot Areas

Two different pilot sites of groundwater-dependent terrestrial ecosystems, namely the Murska šuma lowland oak forest in the northeast and the Krakovski gozd forest in the southeast of Slovenia (Figure 1, Table 1), were selected for our investigations because a high mortality rate, based on at least 25 years of research [16,17] into the physiological state of the trees, was estimated.

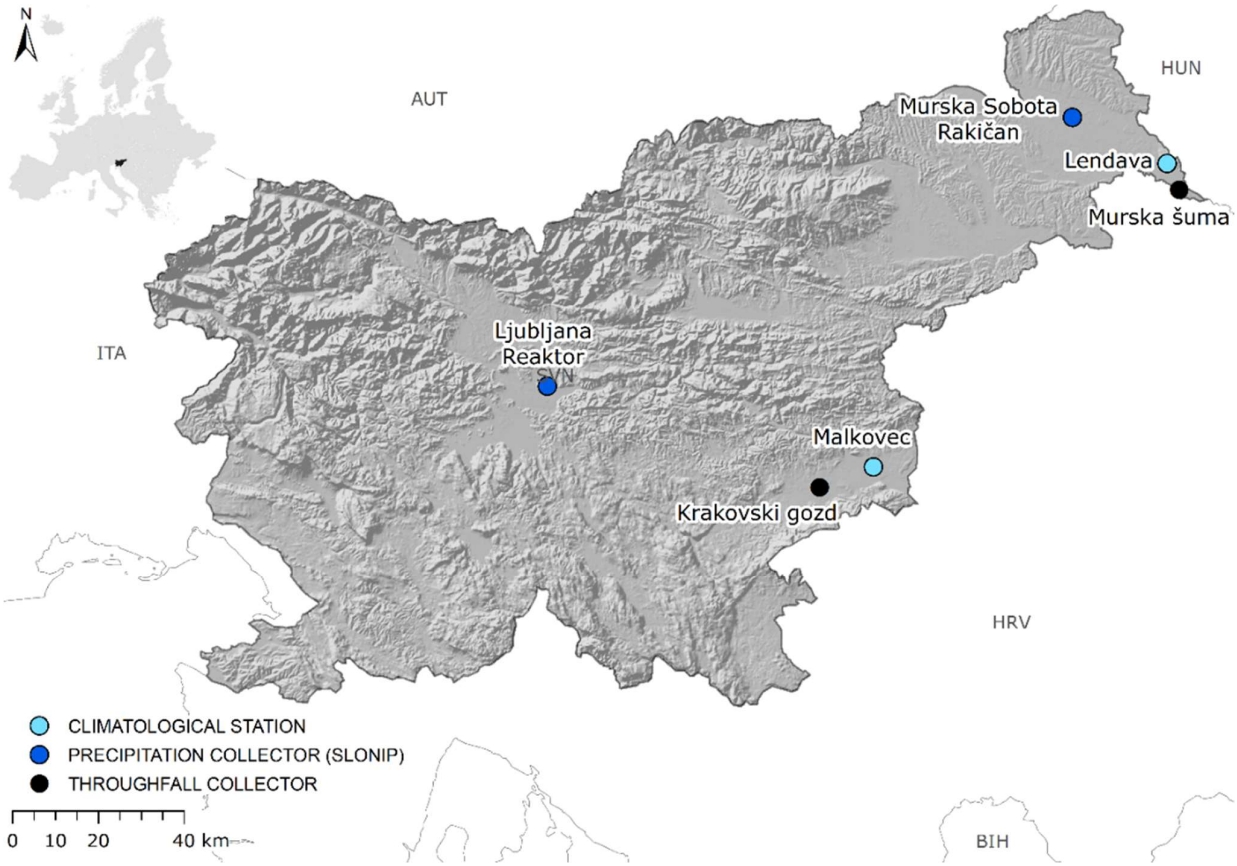

Figure 1. Pilot areas with throughfall collectors at Murska šuma and Krakovski gozd, precipitation collectors at Murska Sobota-Rakičan and Ljubljana-Reaktor stations and Lendava and Malkovec climatological stations included in the research with DEM12.5 [39].

Table 1. Stations equipped with precipitation and throughfall collectors, included in research.

Station Name	Latitude (° N)	Longitude (° E)	Altitude (m.a.s.l.)	Observation Period
Murska šuma [1]	46.4968	16.5129	155.46	July 2021–March 2025
Murska Sobota-Rakičan [2]	46.6520	16.1912	186.00	January 2020–December 2024
Krakovski gozd [1]	45.8822	15.4159	152.89	July 2022–March 2025
Ljubljana-Reaktor [2]	46.0946	14.5970	282.00	January 2020–December 2024

Note: [1] GeoZS—Throughfall collectors; Geological Survey of Slovenia; [2] IJS—SLONIP stations where monitoring is performed by Jožef Stefan Institute [34].

Both pilot areas are lowland alluvial forests, primarily composed of oaks (*Quercus robur* L.), and are protected as nature reserves and Natura 2000 sites. Krakovski gozd is located in the Krško Basin near the Krka River, while Murska šuma is in the Pannonian Basin in the floodplain region along the Mura River. In these two pilot areas, throughfall collectors were installed inside the forests by the Geological Survey of Slovenia (GeoZS) in 2021 and 2022 to observe the isotopic composition of oxygen and hydrogen in throughfall. For further evaluation of the hydrological cycle in the forest, these short-term observations need to be compared with longer-term data from nearby "open space" stations, such as Murska Sobota-Rakičan and Ljubljana-Reaktor [34,35,40].

All four stations (Table 1) are located in a temperate continental climate zone, with differences in annual precipitation range (Murska šuma and Murska Sobota: 800–900 mm, Krakovski gozd 1200–1300 mm, and Ljubljana-Reaktor 1300–1400 mm), but the same annual air temperature range of 10–12 °C (1981–2010) [41].

The Ljubljana-Reaktor station is located approximately 65 km northwest of Krakovski gozd, and the Murska Sobota-Rakičan station is about 30 km northwest of Murska šuma.

To evaluate differences in air temperature and precipitation patterns for the two forest pilot areas, data from the national meteorological monitoring network for the period of 1960–2025 from the two closest climatological stations, Lendava and Malkovec [42], were used (Figure 1, Table 2). Lendava is the closest climatological station to Murska šuma, and Malkovec is the closest to Krakovski gozd.

Table 2. The closest climatological stations to Murska šuma and Krakovski gozd.

Climatological Station	Latitude (° N)	Longitude (° E)	Altitude (m a.s.l.)
Lendava	46.5569	16.4724	190
Malkovec	45.9289	15.5732	150

2.2. Sampling of Precipitation and Throughfall

2.2.1. Precipitation and Throughfall Collectors

The collectors installed in Krakovski gozd and Murska šuma, which collect throughfall, have been custom-built, with a larger opening than the standard Palmex design to prevent clogging by leaves. The containers of the collectors were installed at ground level to limit solar exposure and reduce evaporation. The containers were placed inside an additional plastic barrel for protection. The barrel was covered with a plastic lid and an extra tarpaulin to prevent splash-in contamination from the ground. Monthly throughfall composites were sampled from July 2021 to March 2025 in Murska šuma and from July 2022 to March 2025 in Krakovski gozd.

The precipitation collector installed at Ljubljana-Reaktor has been modified (see Vreča and Malenšek 2016 [35]), whereas at the Murska Sobota station, a classical rain gauge collector is used. In this research, we included data on the isotopic composition of precipitation collected at Murska Sobota-Rakičan and Ljubljana-Reaktor from January 2020 to December 2024 [34,35,40,43].

2.2.2. Sampling Procedures

Sampling in Murska šuma and Krakovski gozd was carried out by GeoZS at the beginning of each month as a monthly composite. The sampling frequency is low when extreme events develop rapidly, so short-term variations may not be fully captured in the observations. More frequent sampling was not feasible due to challenging terrain with dense vegetation and limited accessibility. Automated sampling is also not suitable for this area because of the presence of animals and the associated risk of equipment damage.

Samples from Murska šuma Krakovski gozd, are stored in 50 mL HDPE bottles, transported to the GeoZS laboratory, refrigerated (5–8 °C), filtered (0.45 µm CA), and prepared in 2 mL vials for analysis at GeoZS on a laser isotope analyzer. Monthly composite samples from Murska Sobota–Rakičan and Ljubljana–Reaktor are obtained by emptying event-based collectors into 5–10 L containers and stored at room temperature. Precipitation samples at Ljubljana–Reaktor are collected as soon as possible after each precipitation event by IJS staff, and at Murska Sobota-Rakičan, they are collected daily by ARSO staff using a classical rain gauge collector [34]. In the IJS laboratory, these composites are filtered through 12–25 µm ashless filters to remove particles and stored in glass bottles with a capacity of ≥30 mL at room temperature until analysis on an isotope ratio mass spectrometer [34,35].

2.3. Analysis of Isotopic Composition of Oxygen and Hydrogen

At GeoZS, samples from Murska šuma and Krakovski gozd were analyzed using a Picarro L2130-i laser isotope analyser [43,44], while the samples from Murska Sobota–Rakičan and Ljubljana–Reaktor were analyzed at IJS with a Finnigan MAT DELTA plus dual inlet isotope ratio mass spectrometer [44,45].

The results of analysis obtained by a Picarro L2130-i cavity ring-down spectrometer with a precision of (1δ) 0.03/0.1% for $\delta^{18}O/\delta^{2}H$ [46], were normalized to the international VSMOW–SLAP scale using the reference materials USGS-45 and USGS-47. The internal laboratory reference material W-998 was analyzed together with the samples to monitor measurement repeatability and potential memory effects. Each sample was injected six times, and the first four injections were discarded to minimize memory effects; reported values represent the mean of the final two injections. Data processing, including scale normalization and instrumental drift correction, was performed using LIMS (Laboratory Information Management System for Light Stable Isotopes) for LASERS. Typical drift over 24 h without recalibration is 0.08‰ and 0.3‰ for $\delta^{18}O$ and $\delta^{2}H$, respectively [46].

The results of analysis for Ljubljana-Reaktor and Murska Sobota-Rakičan were obtained by a Finnigan MAT DELTA Plus dual-inlet isotope ratio mass spectrometer (DI-IRMS; Finnigan MAT GmbH, Bremen, Germany) equipped with an automated H_2–H_2O equilibration system [47–49]. Sample equilibration was performed using an HDOeq48 equilibration unit (custom-built by M. Jaklitsch at IAEA, Vienna, Austria). All samples were measured in duplicate together with laboratory reference materials (LRMs). The LRMs were periodically calibrated against the primary VSMOW2 and SLAP2 standards to ensure traceability to the VSMOW–SLAP scale. The results were normalized to the VSMOW–SLAP scale using the LIMS program [45,50].

An interlaboratory comparison was performed using a duplicate throughfall sample from Krakovski gozd (12 July 2024), analyzed in the laboratories of GeoZS and IJS (GeoZS: $\delta^{18}O = -5.52 \pm 0.01$‰, $\delta^{2}H = -33.9 \pm 0.0$‰; IJS: $\delta^{18}O = -5.44 \pm 0.02$‰, $\delta^{2}H = 35.0 \pm 0.0$‰). The measured isotope values differed by 0.08‰ for $\delta^{18}O$ and 1.1‰ for $\delta^{2}H$ (1.74‰ for d-excess), indicating good analytical agreement within the expected analytical uncertainty. Both laboratories also participate in the WICO 2024 intercomparison (IAEA Water Stable Isotope Intercomparison) and show very good analytical performance. Analysis of a six-duplicate sample in both laboratories, on average, resulted in differences of 0.08‰ for

$\delta^{18}O$ and 0.4‰ for $\delta^{2}H$, confirming good interlaboratory agreement within the expected analytical uncertainty.

The collected isotope data are expressed in standard δ notation, representing the relative difference in the isotopic composition of the sample (Rs) with respect to the selected standard (R_{st}) and expressed in parts per million (‰):

$$\delta^{Y}X(‰) = \left(\frac{R_s}{R_{st}} - 1\right) \times 1000 \quad (1)$$

where ^{y}X is oxygen (^{18}O) or hydrogen (^{2}H), and R is the ratio of isotopes $^{18}O/^{16}O$ or $^{2}H/^{1}H$ [51].

The deuterium excess (d-excess) was calculated following Dansgaard (1964) as d-excess [‰] = $\delta^{2}H - 8 \times \delta^{18}O$ [52]. d-excess is widely used to constrain the moisture sources of precipitation, as it primarily depends on relative humidity and sea-surface temperature at the evaporation source, which control molecular diffusion [53,54]. However, d-excess can evolve during vapor transport due to local processes such as sub-cloud evaporation and continental moisture recycling [53]. It shows pronounced seasonality [54–56], with higher values in winter, when relative humidity over the oceans is low, and lower values in summer, when the atmosphere is more humid. Lower humidity enhances kinetic fractionation during evaporation, resulting in higher d-excess in the vapor [53].

2.4. Available Meteorological Data and Its Analysis

Meteorological data from climatological stations, such as air temperature and precipitation, are available on the web portal of the Slovenian Environmental Agency (ARSO) [41]. For the Murska šuma area, data from the Lendava climatological station were used for the analysis. For the Krakovski gozd area, due to data deficiencies, data from the climatological stations Malkovec with Gornji Lenart (1960–1993) and Kostanjevica (1960–1990) were combined and homogenized to remove artificial influences such as station relocations or changes in measurement equipment. Homogenization is carried out by comparing the station's data with nearby stations and mathematically correcting these artificial shifts [57].

The meteorological data comprises daily average, maximum, and minimum temperatures, as well as daily precipitation amounts, for the period 1960 to 2025. For statistical analysis, we divided the data into three periods: 1960–1990, 1991–2020, and 2021–2025. Climate normals are traditionally determined by averaging data over 30 consecutive years [58]. The period 2021–2025 is used because it marks the availability of the first isotopic data for throughfall in these pilot areas.

Using the Statistica program (TIBCO Statistica TM 14.0.0) and MS Excel (pivot tables), we categorized the air temperature and precipitation data for each period by month. With the "Descriptive statistics" function, we calculated the average temperature for each month within a given period and compared these values between periods. We used the Student's t-test [59] to determine the statistical significance between the data from the two periods.

2.4.1. Analysis of Air Temperature and Precipitation Amount

The "warming stripes" are an iconic climate data visualization, adopted globally as a symbol of the warming world, and are created by visualizing long-term temperature data, typically annual average temperatures, as a series of colored vertical stripes arranged chronologically [60]. Each stripe represents one year and is colored according to the temperature anomaly (the difference from an average baseline temperature). The color gradient from blue to red corresponds to temperature deviations relative to a baseline period, with blue indicating years cooler than average and red indicating years warmer

than average. The progression to increasingly intense red hues in recent decades reflects accelerated warming consistent with global climate change.

In our case, warming stripes are constructed using air temperature data for Krakovski gozd (nearest meteorological stations: Cerklje ob Krki and Malkovec [42]) and Murska šuma for the period 1960–2020.

To determine whether there were changes in air temperature and precipitation, we calculated the difference in average air temperature and precipitation between the periods 1991–2020 and 1960–1990. The results are presented as differences within the monthly range.

2.4.2. Extreme Events Analysis

To quantify drought and potential flooding, we calculated the Standardized Precipitation Index (SPI). The SPI values for any given location and accumulation period are classified into seven precipitation classes, ranging from dry to wet, where increasingly severe precipitation deficits (i.e., meteorological droughts) are indicated by SPI values lower than −1.0, while increasingly severe precipitation surpluses are indicated by SPI values above 1.0 [23]. As SPI can be calculated over different precipitation accumulation periods, the resulting values allow for the estimation of various potential impacts of a meteorological drought. When SPI is computed for shorter accumulation periods (e.g., 1 to 3 months), it can be used to support the assessment of reduced soil moisture, snowpack, and flow in smaller creeks, for medium accumulation periods (e.g., 3 to 12 months), it can indicate reduced stream flow and reservoir storage and when for longer accumulation periods (e.g., 12 to 48 months), it can indicate reduced reservoir and groundwater recharge [61].

2.5. Isotope Data

The study includes data from the period between July 2021 (Murska šuma) and March 2025. All isotope data are available in Table S1 (partially in Koren Pepelnik et al. 2025 [43]). Data processing, calculations, and plotting were performed in R Studio version 2025.9.1.401 [62].

2.5.1. Estimation of the Local Meteoric Water Line (LMWL)

The relationship between δ^2H and δ^{18}O values in natural meteoric waters from many regions worldwide has been established, so the isotopic composition relative to ocean water shows a linear correlation across the entire range for waters that have not undergone significant evaporation [47]. When the isotopic composition of precipitation samples from around the world is plotted on δ^{18}O and δ^2H plots, the data form a linear band described by the Global Meteoric Water Line (GMWL) (Equation (2)) [63,64]:

$$(\text{GMWL})\ \delta^2\text{H} = 8 \cdot \delta^{18}\text{O} + 10 \quad (2)$$

GMWL primarily reflects the equilibrium fractionation factors between δ^2H and δ^{18}O in precipitation [52,65]. These factors are influenced by evaporation processes and vary at a local scale, leading to the Local Meteoric Water Lines (LMWL) that usually deviate from the GMWL [66,67]. The distribution of water isotopic composition on a local scale is mainly controlled by air temperature, altitude, distance from the coast, and the amount of precipitation [52,68–70]. Local meteoric water lines (LMWLs) describe the long-term relationship between δ^2H and δ^{18}O in specific regional and local meteorological settings. They serve as a reference for interpreting isotope ratios in terrestrial and biologically derived waters and are useful for hydrological process assessments, aiding in the understanding of water cycle interactions [71]. LMWLs also provide a basis for evaluating isotope-enabled climate models [40].

The determination of the Local Meteoric Water Line (LMWL) uses various regression models. Traditionally, LMWLs are defined using ordinary least squares regression (OLS) or reduced major axis (RMA) regression [67,72]. As RMA is less sensitive to outliers and, more importantly, the relationship between the two assessed variables can be described by physical laws [73], the use of MA or RMA is more appropriate for defining the LMWL [74]. In this research, LMWLs are calculated using different regression methods, including major axis regression (MA), reduced major axis regression (RMA), and precipitation-weighted RMA (PWRMA) as proposed by Hughes and Crawford (2012) [75] and Crawford et al. (2014) [74], and described by Vreča et al. (2024) [45] for multiple Slovenian precipitation stations. PWRMA is most suitable for applications of the LMWL related to groundwater recharge, dam storage, and major flow events; high-magnitude precipitation events are particularly relevant [75]. Therefore, it is appropriate to use an LMWL weighted towards these events, as they often occur during extreme weather conditions, including intense rainfall or extended periods with little or no precipitation.

2.5.2. Seasonal Trends in Isotopic Composition

The typical isotopic seasonal variability shows precipitation is more depleted in heavy isotopes during colder months and more enriched during warmer months. The role of temperature and precipitation amount in controlling isotope seasonality patterns is emphasized [76,77]. Seasonality, defined as the seasonal range or the amplitude (A) of the sine wave of δ^2H and δ^{18}O in precipitation, is useful for interpreting aquifer recharge and groundwater uptake by trees because it reflects temporal variations in the isotopic composition of water inputs to the system [78]. The annual seasonal range can be determined by calculating the difference between the minimum and maximum values of δ^{18}O or δ^2H observed across months or seasons, or by measuring the amplitude of the sine-curve oscillation [52,77,79], using nonlinear least squares [80]. Isotopic compositions of δ^{18}O and δ^2H allow a rough estimate of groundwater mean residence time (MRT). Damping of the sine-curve amplitude oscillation is a method commonly used to calculate MRTs of groundwater [81–83]:

$$\mathrm{MRT} = \frac{\pi}{2}(1 - \mathrm{C})^{\frac{1}{2}} 12/C \quad (3)$$

where C is the amplitude damping given as $C = B/A$, where A is the amplitude of δ^{18}O precipitation values, and B is the amplitude of δ^{18}O values in the groundwater. Using this equation and the amplitude of precipitation (throughfall), we can estimate the MRT of groundwater in the forest area.

3. Results and Discussion

3.1. Air Temperature and Precipitation Amount

Since 1960, the average annual air temperature has gradually increased in the Lendava—Murska šuma (Figure 2A) and Malkovec—Krakovski gozd (Figure 2B) areas.

The trend of increasing air temperature in both areas is not statistically significant ($p > 0.05$) for the period 1960–2020. There is a visible increase in the average annual air temperature, by 0.039–0.042 °C/year (1960–2025) (Figures 2 and 3), which is in average rise of about 2.3–2.5 °C over the last 60 years. This trend is consistent with long-term observations for Slovenia, where mean air temperature increased by approximately 0.36 °C per decade during the period 1961–2011 [84].

Comparison of the periods by counting the number of very hot days (above 25 °C) showed that possible heat stress at both pilot areas became more frequent in the period 1991–2020 (+1.71%; +1.50% of days), and that in this period, there are fewer days when the temperature reached −10 °C (−0.38%; −0.31% of days), which could represent possible cold stress (Figure 4).

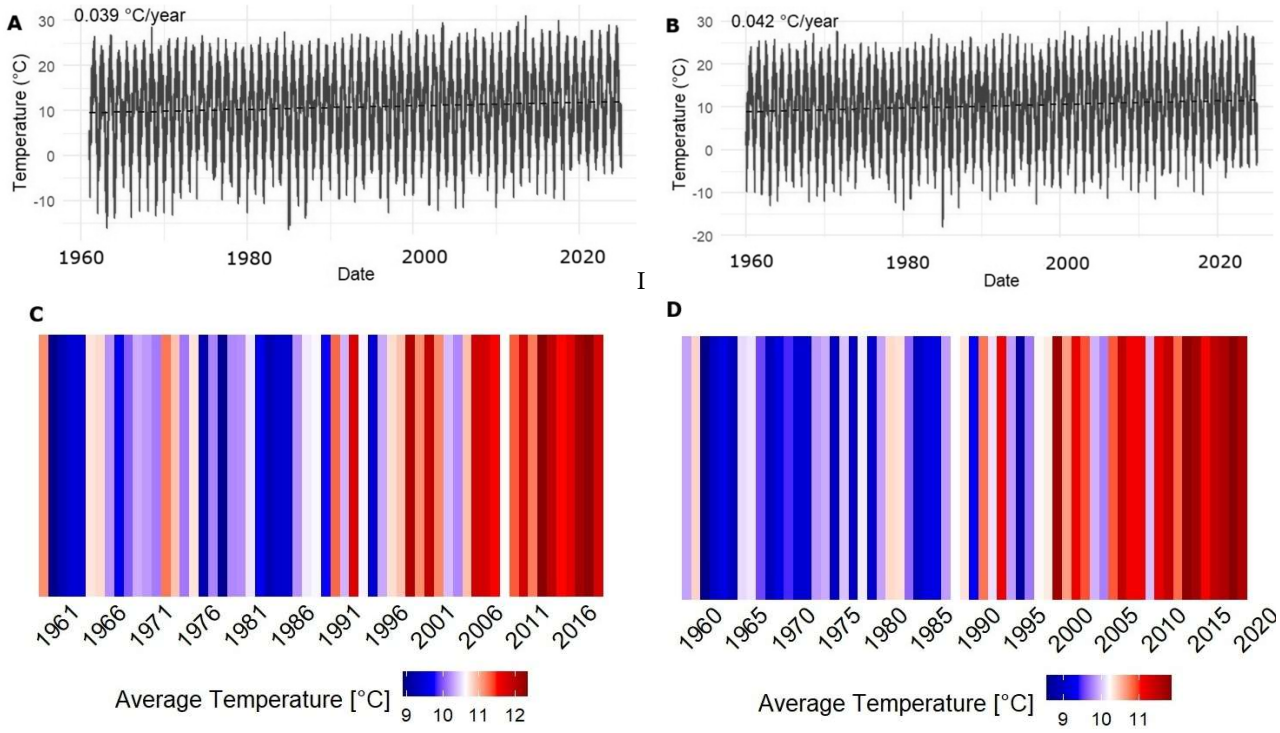

Figure 2. Average air temperature and warming stripes (1960–2020) in Lendava—Murska šuma (**A**,**C**) and Malkovec—Krakovski gozd (**B**,**D**).

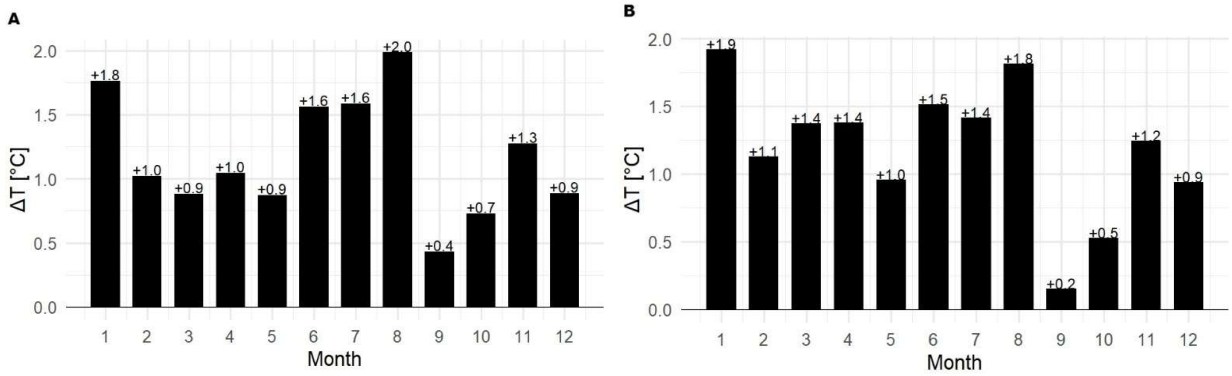

Figure 3. Difference in average monthly air temperature(ΔT) between the periods 1991–2020 and 1960–1990 in Lendava—Murska šuma (**A**) and Malkovec—Krakovski gozd (**B**).

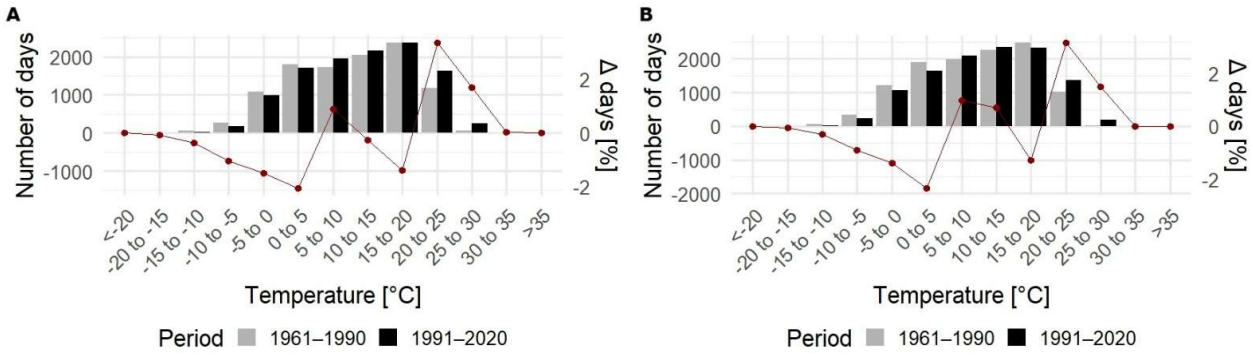

Figure 4. The number of days with average daily temperatures in a particular temperature class during the observation period, and the difference in the proportions of days (dark red line) in Lendava—Murska šuma (**A**) and Malkovec—Krakovski gozd (**B**) between the two periods.

Compared to the period 1960–1990, there is a noticeable decrease in precipitation during the growing season (March–September) in the period 1991–2020, when water needs for trees are high, and an increase in precipitation in the autumn months in both pilot areas (Figure 5). The trend of decreasing total annual precipitation in Lendava—Murska šuma and Malkovec—Krakovski gozd (−0.001 and −0.003 mm/year) in the period 1960–2020 (Figure 6) is statistically significant ($p < 0.05$).

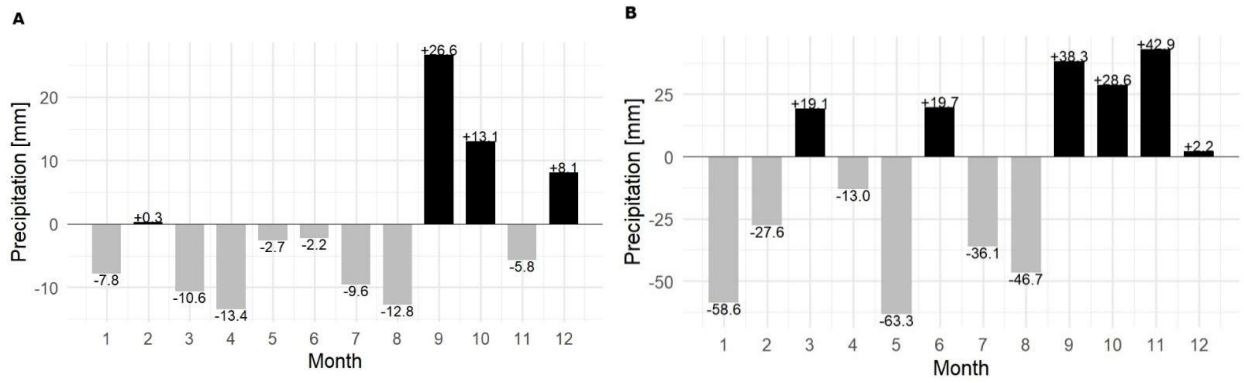

Figure 5. The difference in monthly precipitation amounts between the periods 1991–2020 and 1960–1990 in Lendava–Murska šuma (**A**) and Malkovec—Krakovski gozd (**B**).

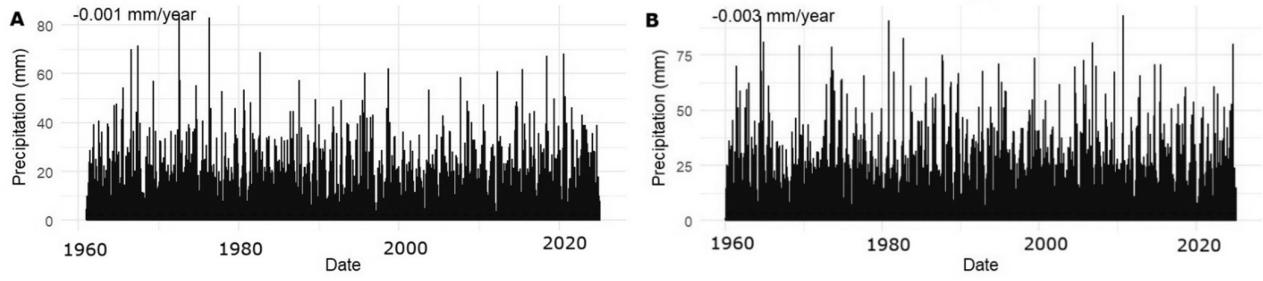

Figure 6. Daily sum of precipitation in the period 1960–2020 in Lendava—Murska šuma (**A**) and Malkovec—Krakovski gozd (**B**).

In Krakovski gozd during the period 1991–2020, the number of days with no precipitation (0 mm/day) increased (+1.50% of days), as did the number of days with daily precipitation of 50 mm (+0.11% of days) (Figure 7). In Murska šuma, the number of days with precipitation between 0.1 and 10 mm/day increased by +0.51% of days during the period 1991–2020, while the number of days with daily precipitation of 50 mm increased by 0.01% of days, and those with 70 mm increased by 0.04% of days.

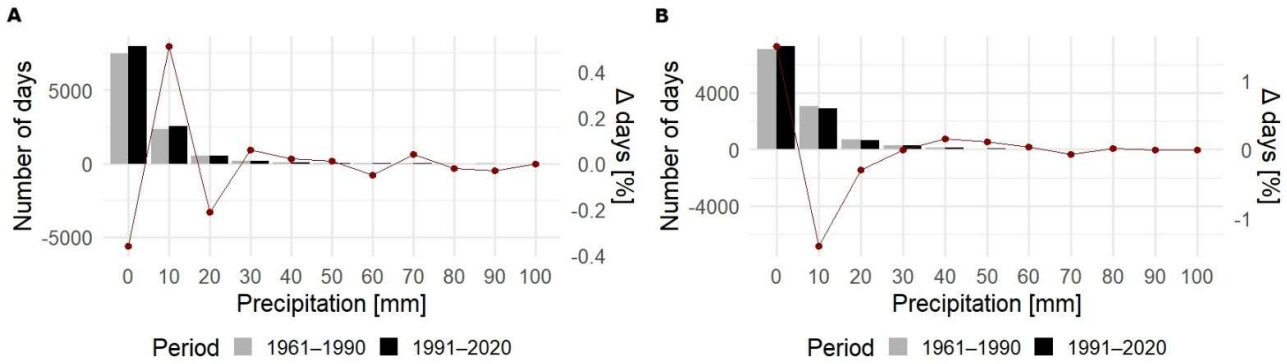

Figure 7. Number of days in both periods in Lendava—Murska šuma (**A**) and Malkovec—Krakovski gozd (**B**) by individual precipitation classes, and the change between the two periods in terms of the change in the proportion of days (dark red line).

The extreme events in 2022 (drought) (SPI 12, 24 < −1) and 2023 (flood) (SPI 3, 12 > 1) are evident, especially when observing the 3-month and 12-month SPI (Figure 8). In the year 2022, meteorological and hydrological drought was confirmed [85], with some periods experiencing no precipitation for a month or more. In contrast, at the beginning of August 2023, the northern and eastern parts of Slovenia experienced extreme floods [24].

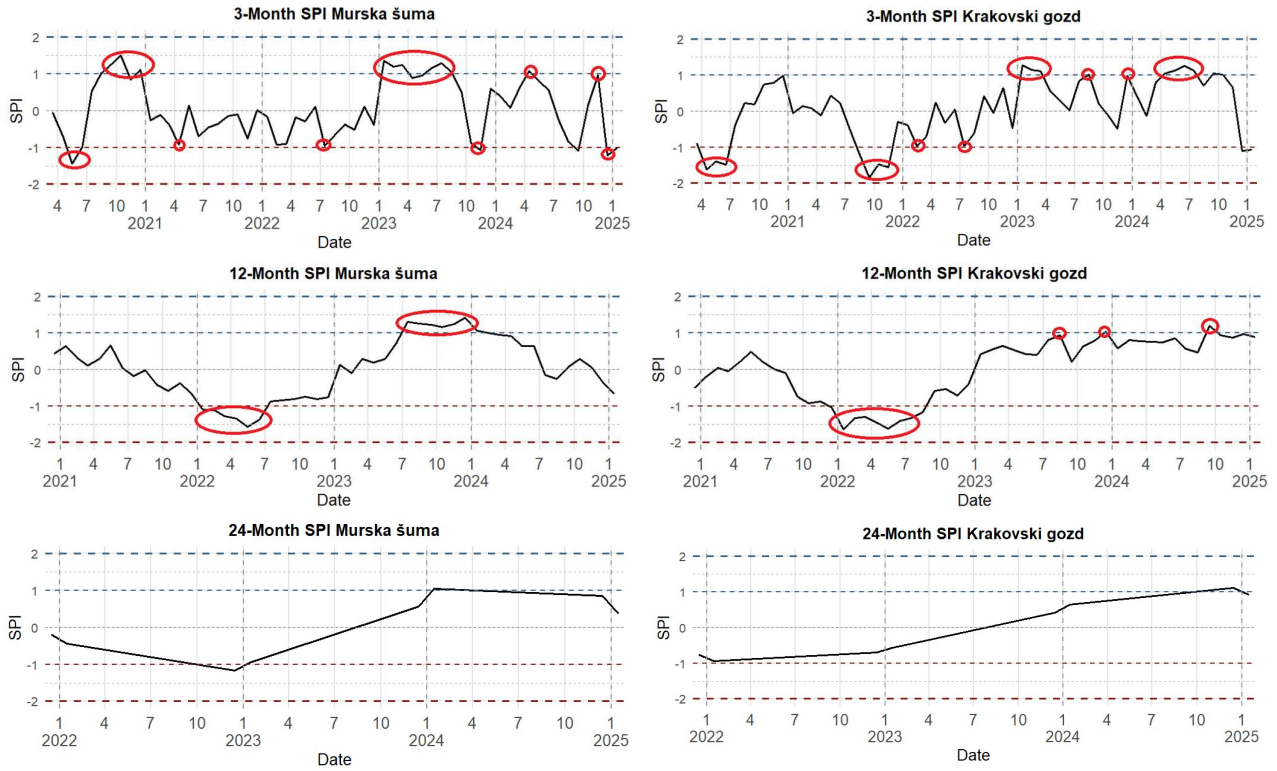

Figure 8. SPI for accumulation periods of 3, 12, and 24 months.

3.2. Stable Isotope Composition of Throughfall

These extreme events can be identified by comparing air temperature and precipitation amounts (Figure 9), as well as the isotopic composition of oxygen and hydrogen in precipitation (δ^{18}O, δ^{2}H, deuterium excess) (Figure 10) in both forest areas.

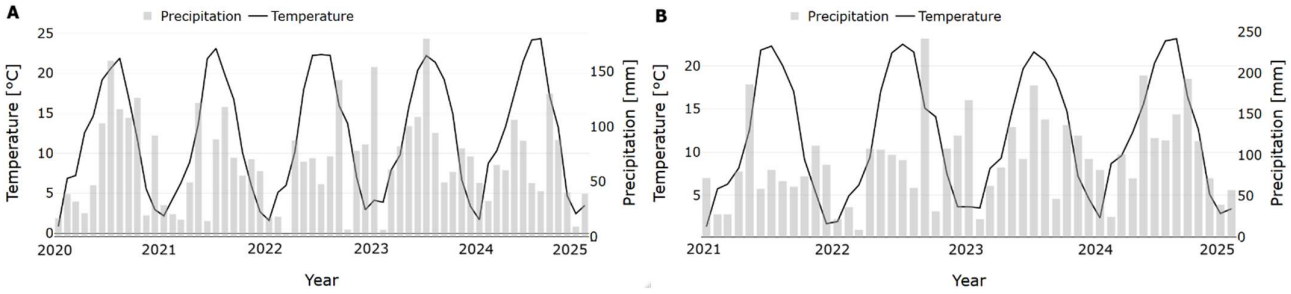

Figure 9. Average seasonal air temperature and monthly precipitation amount in years 2021–2025 in Lendava—Murska šuma (**A**) and Malkovec—Krakovski gozd (**B**).

The seasonal amplitude depends on changes in air temperature and in the origin of the air masses and secondary processes that influence the original isotopic composition of precipitation.

The monthly variability of δ^{2}H and δ^{18}O (Figure 10A,B) shows a clear seasonal pattern, with more depleted values during the winter (dormant season) and enriched values during the summer (growing season). This pattern is characteristic of continental precipitation

regimes and is consistent with observations from nearby monitoring stations such as Ljubljana [86–88] and Zagreb [89].

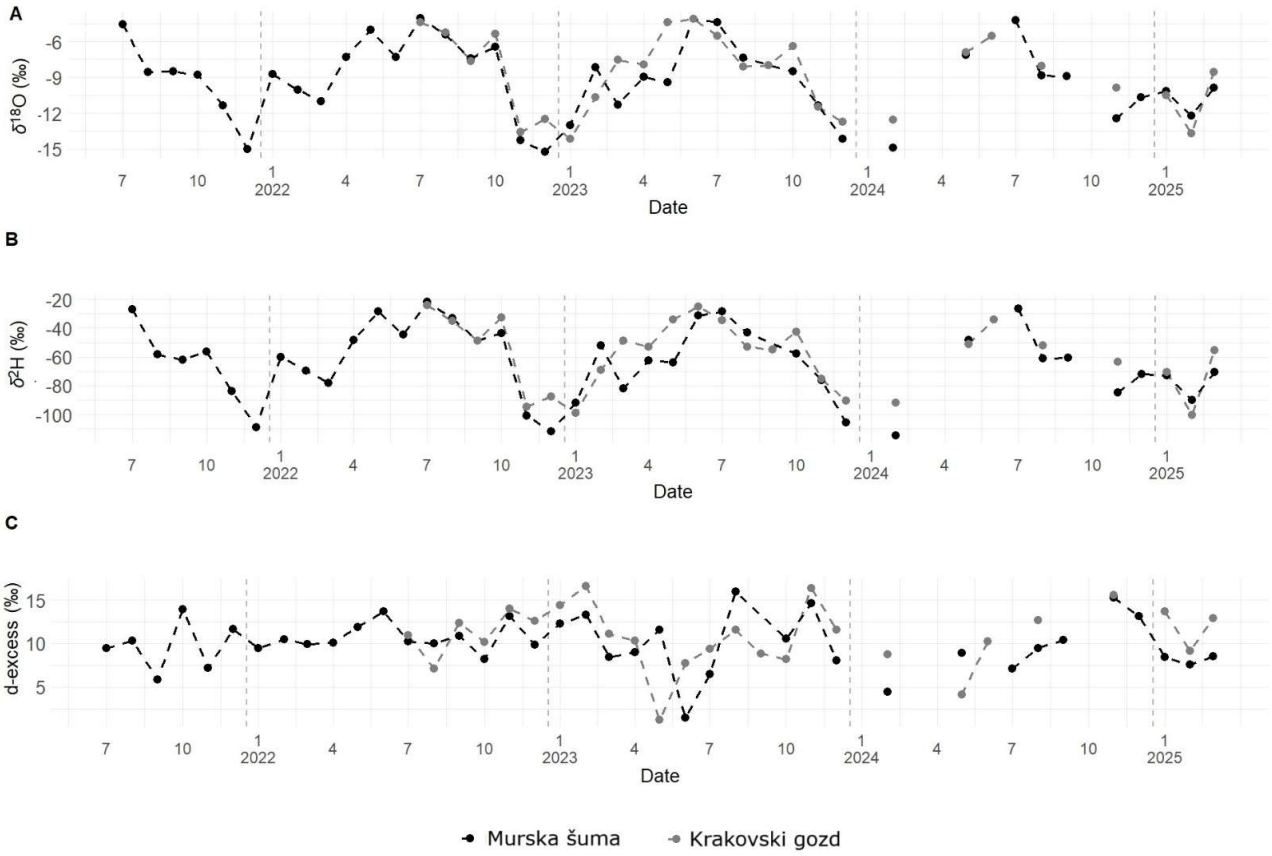

Figure 10. The isotopic composition of oxygen and hydrogen in throughfall (δ^{18}O (**A**), δ^{2}H (**B**), deuterium excess (**C**)) in Murska šuma and Krakovski gozd.

The lowest monthly δ^{2}H values in throughfall were recorded during the dormant season, reaching −114.7‰ in February 2024 at Murska šuma and −100.6‰ in February 2025 at Krakovski gozd. The highest δ^{2}H values occurred during the growing season, with −22.0‰ in July 2022 at Murska šuma and −24.2‰ in July 2022 at Krakovski gozd. A similar seasonal signal is observed in precipitation. The most depleted δ^{2}H values were measured in the dormant season (−113.8‰ in February 2024 at Murska Sobota–Rakičan and −99.2‰ in November 2020 at Ljubljana–Reaktor), while the most enriched values occurred in the growing season (−17.5‰ in July 2022 at Murska Sobota–Rakičan and −27.0‰ in July 2021 and July 2024 at Ljubljana–Reaktor).

The δ^{18}O record follows the same seasonal pattern as δ^{2}H. In throughfall, the lowest δ^{18}O values were recorded during the dormant season (−15.22‰ in December 2021 at Murska šuma and −14.18‰ in January 2023 at Krakovski gozd). The highest values occurred during the growing season, reaching −4.02‰ in July 2022 at Murska šuma and −4.10‰ in June 2023 at Krakovski gozd. Precipitation shows comparable seasonal variability, with the lowest δ^{18}O values recorded during the dormant season (−15.34‰ in December 2021 at Murska Sobota–Rakičan and −13.44‰ in November 2020 at Ljubljana–Reaktor) and the highest during the growing season (−4.21‰ in August 2024 at Murska Sobota–Rakičan and −2.73‰ in July 2022 at Ljubljana–Reaktor).

The d-excess in throughfall shows greater variability than the isotope ratios themselves. The lowest values were observed during the growing season (1.24‰ in May 2023 at Krakovski gozd and 1.47‰ in June 2023 at Murska šuma). The highest d-excess values occurred in different seasons at the two sites, reaching 15.9‰ in August 2023 at Murska

šuma and 16.6‰ in February 2023 at Krakovski gozd. In precipitation, the lowest d-excess values were recorded during the dormant season at Murska Sobota–Rakičan (2.4‰ in October 2022 and February 2024) and during the growing season at Ljubljana–Reaktor (2.7‰ in June 2021 and August 2022). The highest d-excess values in precipitation were recorded in the dormant season (16.3‰ in December 2024 at Murska Sobota–Rakičan and 18.0‰ in February 2023 at Ljubljana–Reaktor). The $\delta^{18}O$, $\delta^{2}H$, and d-excess values of nearby Ljubljana precipitation are increasing (+0.02‰, +0.18‰, and +0.05‰ per year, respectively), consistent with regional warming estimated to 0.069 °C/year [40]. The values of d-excess throughout 2022 at Murska šuma exhibit low variability during the drought period (Figure 10C). In 2023, during the flood period, the d-excess values in August are the highest recorded in the entire observation period, while before the flood, the values are extremely low (May and June 2023) (Figure 10C). Similar fluctuations are observed at Krakovski gozd. Higher d-excess values (15‰ to 25‰) are often associated with moisture originating from oceanic sources with limited evaporation or direct marine influence [90] or contribution from terrestrial moisture recycling [91–93].

More positive values of $\delta^{18}O$ and $\delta^{2}H$ during the growing season are expected, due to higher air temperatures compared to the dormant, autumn–winter seasons when air temperatures are lower. In 2022, a drought period was identified, and the $\delta^{18}O$ and $\delta^{2}H$ values in the growing season were the most positive for the entire observation period (Murska šuma 2022: $\delta^{18}O = -4.02‰$, $\delta^{2}H = -22.0‰$). The ranges (variability) of d-excess in both the growing and dormant seasons were also the smallest. The stronger influence of sub-cloud processes on the weaker rains, which mainly occurs in drier and warmer months when evaporation of falling droplets is more likely, is evident in the more positive $\delta^{18}O$ values [53,94]. In 2023, during the flood period, the range between $\delta^{18}O$ and $\delta^{2}H$ values in the growing season is the largest. The d-excess in both forests during the 2023 growing season reaches the lowest values of the entire observation period (1.2 and 1.7‰). The low d-excess values during the wet season indicate the moisture transported from long distances [95]. The low d-excess values can be attributed either to the evaporation of raindrops from the surface of the rain gauge at lower relative humidity [45,96], or to secondary processes such as partial evaporation of raindrops below the cloud base [45,97]. The increased precipitation contribution in autumn, the dormant season over the last 30 years in Murska šuma and Krakovski gozd (Figures 5 and 6), is potentially due to a significant contribution of Mediterranean-sourced air masses or contribution from terrestrial moisture recycling to autumn precipitation, as indicated by elevated d-excess values during autumn [40]. More detailed investigations are needed in the future for the identification of specific processes. This suggests an accelerating, exponential isotopic response to warming that has already influenced the water cycle, providing isotopic evidence that interactions among precipitation, surface water, and groundwater in the investigated region have changed over the past decade [40,83].

Figure 11 shows the isotopic composition of throughfall in both forests during the growing (March–September) and dormant (October–February) seasons for the period 2021–2025; in 2025, data are only for the dormant season.

The constructed sine curve and estimated amplitude of seasonality (Figure 12), along with the LMWL of Murska šuma and Krakovski gozd (Table 3), are useful tools for the subsequent steps. Here, the isotopic composition of other matrices (e.g., surface water, xylem, soil water, groundwater) can be represented in a $\delta^{18}O/\delta^{2}H$ plot to quantify the root water uptake from different soil layers or groundwater by comparing isotope ratios in soil profiles, groundwater, and xylem water. This is often achieved using graphical approaches (with LMWL) or mixing models and is also used for partitioning water sources in trees.

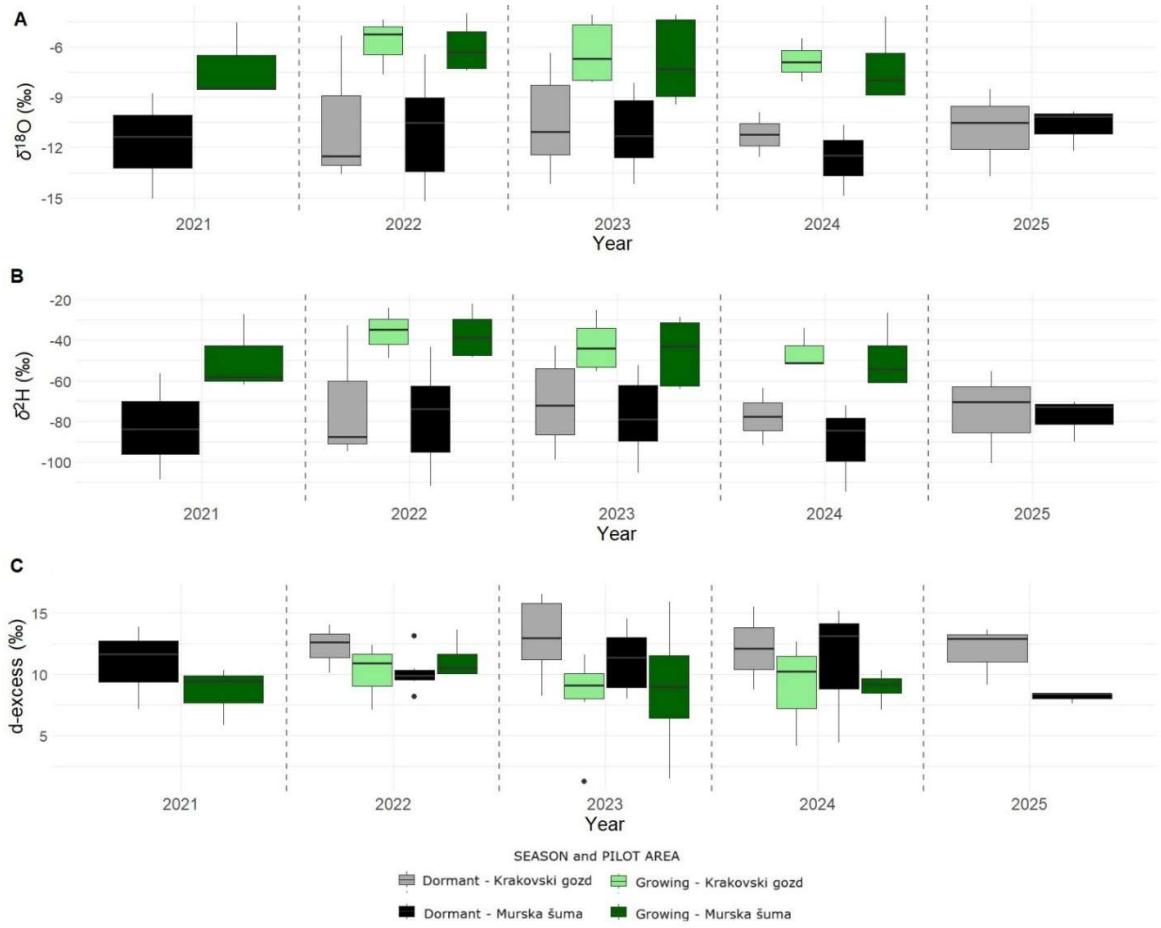

Figure 11. The isotopic composition of oxygen and hydrogen in throughfall (δ^{18}O (**A**), δ^{2}H (**B**), deuterium excess (**C**)) during the dormant and growing seasons in the pilot areas of Murska šuma and Krakovski gozd.

Table 3. Slope and intercept of the LMWLs for the Murska šuma and Krakovski gozd forests, and the SLONIP nearby stations Murska Sobota-Rakičan and Ljubljana-Reaktor.

Station/Method	MA	PWMA	PWRMA	MA	PWMA	PWRMA
		Slope			Intercept	
Murska šuma (July 2021–March 2025)	8.00	7.94	7.89	10.2	9.6	9.1
2022—drought	7.97	7.91	7.90	10.3	10.0	9.9
2023—flood	7.67	7.67	7.61	7.0	7.0	6.4
Murska Sobota-Rakičan (January 2020–December 2024)	7.79	7.77	7.74	7.6	8.1	7.8
2022—drought	7.76	7.88	7.86	7.7	9.5	9.4
2023—flood	7.76	7.80	7.78	6.9	7.8	7.6
Krakovski gozd (July 2022–March 2025)	7.42	7.33	7.26	5.7	5.3	4.7
2022—drought *	7.45	7.62	7.62	6.4	8.7	8.6
2023—flood	7.09	7.18	7.15	2.9	3.5	3.2
Ljubljana-Reaktor (January 2020–December 2024)	7.49	7.54	7.49	6.7	7.6	7.2
2022—drought	7.15	7.26	7.20	3.5	5.6	5.1
2023—flood	7.86	7.86	7.82	10.6	10.4	10.1

Note: * monitoring started in July 2022.

The δ^{18}O one year amplitudes (Figure 12) in Murska šuma (July 2021–March 2025; $\delta^{18}O = -9.02 + 0.04 \sin + 3.61 \cos$; A = 3.61‰) and Krakovski gozd (July 2022–March 2025; $\delta^{18}O = -8.54 + 0.05 \sin + 3.71 \cos$; A = 3.71‰) show the variability in isotopic composition in throughfall between winter (depleted in heavier isotopes) and summer (enriched in heavier isotopes), and quantify the strength of seasonal cycles as deviations from the average annual

value [79]. The variability in precipitation is also seen in Ljubljana-Reaktor (January 2020–December 2024; $\delta^{18}O = -8.03 + 0.16 \sin + 2.67 \cos$; A = 2.67‰) and Murska Sobota-Rakičan (January 2020–December 2024; $\delta^{18}O = -9.04 + 0.14 \sin + 3.81 \cos$; A = 3.81‰).

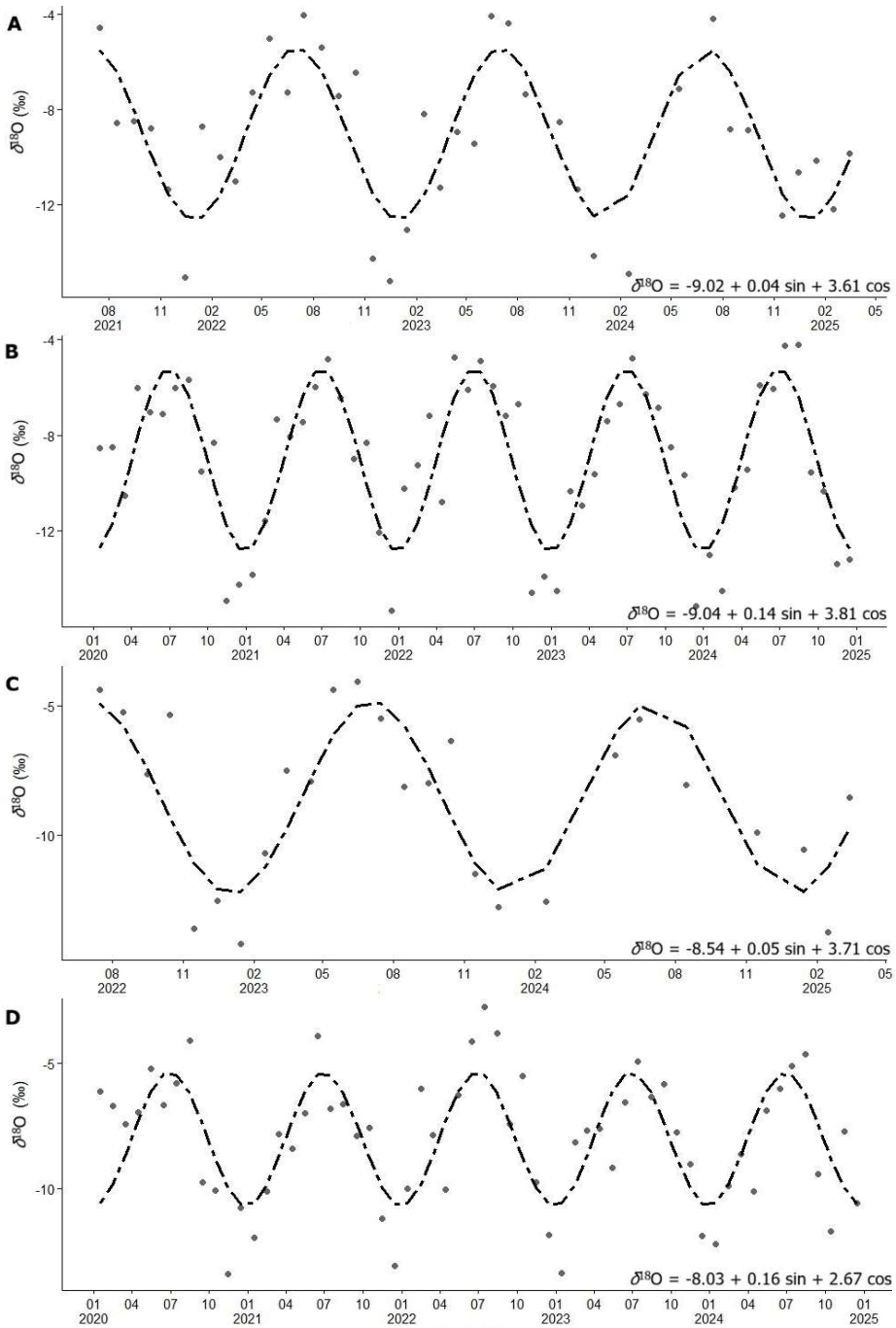

Figure 12. Seasonal sine curve fit of isotopic composition of $\delta^{18}O$ of throughfall in Murska šuma (**A**) and Krakovski gozd (**C**) and precipitation in Murska Sobota-Rakičan (**B**) and Ljubljana-Reaktor (**D**).

The LMWLs for Murska šuma and Krakovski gozd are obtained using three different regression methods (MA, PWMA, and PWRMA) and are presented for comparison with nearest open space monitoring stations together with LMWLs for Murska Sobota-Rakičan and Ljubljana-Reaktor in Table 3. In the case of describing extreme events as drought and floods, influenced by the amount of precipitation, the most suitable LMWL in our case is the one obtained by PWRMA regression, which accounts for analytical uncertainty in both $\delta^{18}O$ and $\delta^{2}H$ and the hydrological importance of precipitation amount.

Spatial variations in LMWL slopes, therefore, provide information on seasonal climatology and are commonly used to infer the seasonality of groundwater recharge and soil water uptake by plants [10,38,54,59,63]. The $LMWL_{PWRMA}$ slope over a period of four years at Murska šuma and Murska Sobota-Rakičan is very similar (7.89; 7.74) to the slope of the GMWL [54]; in comparison with the GMWL, the slope at Krakovski gozd and Ljubljana-Reaktor differs by 0.51–0.74‰ (7.26; 7.49). Minor deviations from the GMWL slope suggest limited evaporation during moisture transport from the ocean to the precipitation site [59,79]. Slopes differing from 8 may also reflect precipitation formed under non-equilibrium conditions in at least one season, which can be assessed using the deuterium-excess parameter. The $LMWL_{PWRMA}$ in Murska šuma, Murska Sobota-Rakičan, and Krakovski gozd for the year 2022 (drought) deviates from the long-term $LMWL_{PWRMA}$ and GMWL by having a higher intercept and slope, showing possible increased sub-cloud evaporation or lower relative humidity [71,98], which preferentially enriches $\delta^{18}O$ relative to $\delta^{2}H$ (reducing slope). In Ljubljana-Reaktor, for the year 2022, the slope and intercept are lower in comparison with the long-period slope and intercept. Previous investigation indicated that the LMWL for Ljubljana for 2007–2010 was close to the GMWL [86]; however, comparing the LMWL for Ljubljana to this study for the period 2020–2024 (slope: 7.49; intercept: 7.2) and previous research for the period 2020–2021 (slope: 8.09; intercept: 10.6) [83], a significant difference in time can be observed for the intercept and slope. In addition, differences in the line intercepts are present due to regional environmental factors, and can be attributed to warmer summer and winter months compared to the long-term mean [83]. The difference in isotopic composition between open-site precipitation and throughfall is most pronounced in summer and results from canopy interception and related modification processes in forest environments, including evaporation, isotopic exchange, and selective retention, which together enrich throughfall in heavy isotopes [44].

At Krakovski gozd, the most depleted values plotting above the GMWL are associated with precipitation from mixed-phase clouds [71]. In contrast, enriched values above the GMWL during months with low precipitation amounts indicate the influence of continental moisture recycling [71]. Enriched values below the GMWL reflect sub-cloud evaporation, a process enhanced under low relative humidity and high air temperature. Sub-cloud evaporation preferentially affects small raindrops, leading to isotopic enrichment of precipitation during descent, and may prevent very small droplets from reaching the ground [71,99].

3.3. Policy Implications

The findings of this research underscore the importance of integrating groundwater-dependent terrestrial ecosystems (GDTEs), such as phreatophytic forests, into strategic groundwater management. As these ecosystems are highly sensitive to groundwater level fluctuations, especially with increasing climate variability and more frequent droughts, groundwater abstraction and land-use planning should consider ecosystem water requirements alongside human demands [100]. Stable isotope analyses of precipitation and plant water are important tools for identifying the sources of water used by vegetation and for distinguishing between groundwater and soil water uptake. These approaches enhance the understanding of ecosystem dependence on groundwater and support the identification of critical groundwater thresholds. In accordance with the European Water Framework Directive [101,102], incorporating these insights into groundwater governance and climate adaptation strategies is essential for maintaining the ecological functioning and resilience of groundwater-dependent ecosystems [100].

4. Conclusions

This work presents the first systematic analysis of changes in air temperature and precipitation amount over the past 65 years in two Slovenian lowland forests, Murska šuma and Krakovski gozd, aligned with research on the isotopic composition of throughfall as a valuable tool for studying forest hydrology dynamics, particularly during extreme events. Climate changes at these two sites are evident in the rise in air temperature of approximately 2.5 °C in 60 years. The decrease in total precipitation amount over the last 65 years is negligible (less than 0.1 mm), but there are clear changes in precipitation patterns over the past 35 years, with a decrease in the amount of precipitation during the growing season and an increase during the dormant season.

This change is also evident in the isotopic composition of precipitation and throughfall, with deuterium excess in the autumn–winter season, indicating a significant contribution from air masses originating in the Mediterranean Sea. Seasonal $\delta^{18}O$ and $\delta^{2}H$ patterns reflect climate-driven variability in moisture sources. Changes in precipitation patterns, related to altered infiltration dynamics, may impair water availability for trees, especially during drought.

The drought in 2022 and the flood in 2023 are confirmed by the calculated SPI values and are also reflected in the isotopic composition of throughfall. During the growing season of 2023, at the time of flood, the d-excess in both forests reaches the lowest values of the entire observation period (1.2 and 1.7‰), indicating the moisture transported from long distances. As in 2022, the drought period was estimated; the values of $\delta^{18}O$ and $\delta^{2}H$ during the growing season are the most positive compared to the entire observation period, and the variability of d-excess in the growing and dormant seasons of 2022 is the smallest. Seasonal variability is further demonstrated by the sinusoidal fit of throughfall isotopic data. The sine curves constructed for throughfall at Krakovski gozd and Murska šuma show amplitudes of 3.71‰ and 3.61‰, respectively, for the period from July 2021 and July 2022 to March 2025, and are comparable with the amplitude for Murska Sobota-Rakičan open space isotope in precipitation monitoring stations, but the amplitude for Ljubljana differs markedly compared to the remaining three amplitudes.

Understanding isotopic variability in precipitation is essential for assessing future water availability under climate change. The known amplitudes of throughfall, together with groundwater isotope amplitudes, contribute to estimating mean residence time (MRT), a key parameter for groundwater management and for integrating groundwater-dependent ecosystems, such as these two forest sites, into strategic groundwater planning. It remains unclear whether increased tree mortality is primarily related to dependence on shallow soil water, which is strongly influenced by precipitation, or on groundwater deeper than 1.5 m below ground surface. Identifying the dominant water source used by trees during extreme events would allow better assessment of the main stress drivers and the amount of water required for tree survival during such periods. Therefore, concurrent sampling of xylem water and other potential water sources is necessary to determine water source partitioning.

Supplementary Materials: The following supporting information can be downloaded at: https://www.mdpi.com/article/10.3390/w18060760/s1, Table S1. Metadata and results.

Author Contributions: Conceptualization: K.K.P. and P.V.; methodology: K.K.P. and P.V.; formal analysis: K.K.P. and P.V.; investigation: K.K.P. and P.V.; data curation: K.K.P. and P.V.; writing—original draft preparation: K.K.P.; writing—review and editing: K.K.P., M.J., M.Č., B.Č.C. and P.V.; visualization: K.K.P.; supervision: M.J., M.Č., B.Č.C. and P.V.; project administration: P.V.; funding acquisition: K.K.P. and P.V. All authors have read and agreed to the published version of the manuscript.

Funding: Activities of this research were funded in last decade by the Research core funding P4-0107 Program research at the Slovenian Forestry Institute, European Regional Development Fund, Interreg

Danube Project SCAN-DANUBE DRP0300848, by the Slovenian Research Agency and Innovation Agency (research core funding P1-0143, P1-0195, N1-0054, N1-0309 and P1-0020), IAEA projects (CRP F31006, TC RER7013, TC RER7017, SLO7001), and projects Mladi forum and FREYA, which are co-funded by the Slovenian Research and Innovation Agency within the framework of Developmental fund pillar.

Data Availability Statement: The data of the isotopic composition of precipitation and throughfall used in this research are available in the Supplementary Materials Table S1 and at: https://doi.org/10.5281/zenodo.17723128.

Acknowledgments: We thank Miroslav Medić, Jan Udovč, and Blaž Pucihar for water sampling for many years. Also, thanks to Aljaž Ciglar, Klara Žagar, and Stojan Žigon for help with isotope analysis. The authors have reviewed and edited the output and take full responsibility for the content of this publication.

Conflicts of Interest: The authors declare no conflicts of interest.

References

1. Reddington, C.L.; Smith, C.; Butt, E.W.; Baker, J.C.A.; Oliveira, B.F.A.; Yamba, E.I.; Spracklen, D.V. Tropical Deforestation Is Associated with Considerable Heat-Related Mortality. *Nat. Clim. Change* **2025**, *15*, 992–999. [CrossRef] [PubMed]
2. Trifković, V.; Ficko, A. Background Mortality in Even- and Uneven-Aged Stands under Climate Change: Insights from 1.4 Million Trees in Slovenia. *For. Ecol. Manag.* **2025**, *594*, 122955. [CrossRef]
3. Calvin, K.; Dasgupta, D.; Krinner, G.; Mukherji, A.; Thorne, P.W.; Trisos, C.; Romero, J.; Aldunce, P.; Barrett, K.; Blanco, G.; et al. *IPCC, 2023: Climate Change 2023: Synthesis Report. Contribution of Working Groups I, II and III to the Sixth Assessment Report of the Intergovernmental Panel on Climate Change*; Core Writing Team, Lee, H., Romero, J., Eds.; IPCC: Geneva, Switzerland, 2023.
4. Knutzen, F.; Averbeck, P.; Barrasso, C.; Bouwer, L.M.; Gardiner, B.; Grünzweig, J.M.; Hänel, S.; Haustein, K.; Johannessen, M.R.; Kollet, S.; et al. Impacts and Damages of the European Multi-Year Drought and Heat Event 2018–2022 on Forests, a Review. *EGUsphere* **2023**. [CrossRef]
5. Layritz, L.S.; Gregor, K.; Krause, A.; Kruse, S.; Meyer, B.F.; Pugh, T.A.M.; Rammig, A. DisentanglingFuture Effects of Climate-Change and Forest Disturbance on Vegetation Composition and Land Surface Properties of the Boreal Forest. *Biogeosciences* **2025**, *22*, 3635–3660. [CrossRef]
6. Anderson-Teixeira, K.J.; Miller, A.D.; Mohan, J.E.; Hudiburg, T.W.; Duval, B.D.; DeLucia, E.H. Altered Dynamics of Forest Recovery under a Changing Climate. *Glob. Change Biol.* **2013**, *19*, 2001–2021. [CrossRef]
7. Larjavaara, M.; Muller-Landau, H.C. Temperature Explains Global Variation in Biomass among Humid Old-Growth Forests. *Glob. Ecol. Biogeogr.* **2012**, *21*, 998–1006. [CrossRef]
8. Kriegler, E.; Edenhofer, O.; Reuster, L.; Luderer, G.; Klein, D. Is Atmospheric Carbon Dioxide Removal a Game Changer for Climate Change Mitigation? *Clim. Change* **2013**, *118*, 45–57. [CrossRef]
9. Barnes, M.L.; Zhang, Q.; Robeson, S.M.; Young, L.; Burakowski, E.A.; Oishi, A.C.; Stoy, P.C.; Katul, G.; Novick, K.A. A Century of Reforestation Reduced Anthropogenic Warming in the Eastern United States. *Earth's Future* **2024**, *12*, e2023EF003663. [CrossRef]
10. Schlesinger, W.H.; Jasechko, S. Transpiration in the Global Water Cycle. *Agric. For. Meteorol.* **2014**, *189*, 115–117. [CrossRef]
11. Fajon Kovač, M.Š.; Vilhar, U.; Ferreura, A. *Gozd in Voda; Rezultati Projekta Interreg III A*; Slovenian Forestry Institute and Slovenia Forest Service: Ljubljana, Slovenia, 2007.
12. Gupta, S.K.; Ram, J.; Singh, H. Comparative Study of Transpiration in Cooling Effect of Tree Species in the Atmosphere. *J. Geosci. Environ. Prot.* **2018**, *6*, 151–166. [CrossRef]
13. Hayat, M.; Xu, X.; Liu, R. Hydroclimatic Constraints on Tree Transpiration-Induced Cooling Across Global Biomes. *Geophys. Res. Lett.* **2025**, *52*, e2024GL113551. [CrossRef]
14. Winbourne, J.B.; Jones, T.S.; Garvey, S.M.; Harrison, J.L.; Wang, L.; Li, D.; Templer, P.H.; Hutyra, L.R. Tree Transpiration and Urban Temperatures: Current Understanding, Implications, and Future Research Directions. *BioScience* **2020**, *70*, 576–588. [CrossRef]
15. Li, Y.; Brando, P.M.; Morton, D.C.; Lawrence, D.M.; Yang, H.; Randerson, J.T. Deforestation-Induced Climate Change Reduces Carbon Storage in Remaining Tropical Forests. *Nat. Commun.* **2022**, *13*, 1964. [CrossRef]
16. Čater, M.A. 20-Year Overview of Quercus Robur, L. Mortality and Crown Conditions in Slovenia. *Forests* **2015**, *6*, 581–593. [CrossRef]
17. Čater, M.; Batič, F. Groundwater and Light Conditions as Factors in the Survival of Pedunculate Oak (*Quercus robur* L.) Seedlings. *Eur. J. For. Res.* **2006**, *125*, 419–426. [CrossRef]
18. Senf, C.; Pflugmacher, D.; Zhiqiang, Y.; Sebald, J.; Knorn, J.; Neumann, M.; Hostert, P.; Seidl, R. Canopy Mortality Has Doubled in Europe's Temperate Forests over the Last Three Decades. *Nat. Commun.* **2018**, *9*, 4978. [CrossRef]

19. Senf, C.; Buras, A.; Zang, C.S.; Rammig, A.; Seidl, R. Excess Forest Mortality Is Consistently Linked to Drought across Europe. *Nat. Commun.* **2020**, *11*, 6200. [CrossRef] [PubMed]
20. Types of Drought | National Drought Mitigation Center. Available online: https://drought.unl.edu/Education/DroughtIn-depth/TypesofDrought.aspx (accessed on 23 December 2025).
21. Wilhite, D.A.; Glantz, M.H. Understanding: The Drought Phenomenon: The Role of Definitions. *Water Int.* **1985**, *10*, 111–120. [CrossRef]
22. Agricultural Droughts | Okoljski Kazalci. Available online: https://kazalci.arso.gov.si/en/content/agricultural-droughts-1 (accessed on 22 December 2025).
23. Svoboda, M.H.M.; Wood, D. *Standardized Precipitation Index User Guide*; World Meteorological Organization: Geneva, Switzerland, 2012.
24. Bezak, N.; Panagos, P.; Liakos, L.; Mikoš, M. Brief Communication: A First Hydrological Investigation of Extreme August 2023 Floods in Slovenia, Europe. *Nat. Hazards Earth Syst. Sci.* **2023**, *23*, 3885–3893. [CrossRef]
25. Šraj, M.; Lah, A.; Brilly, M. Measurements and Analysis of Intercepted Precipitation of Silver Birch (*Betulapendula* Roth.) and Scots Pine (*Pinus sylvestris*, L.) in Urban Area. *Gozdarski Vesn.* **2008**, *66*, 406–433.
26. Zabret, K. The Influence of Tree Characteristics on Rainfall Interception. *Acta Hydrotech.* **2013**, *26*, 99–116.
27. Ogunfolaji, Y.O.; Alivio, M.B.; Orosz, K.; Herceg, A.; Kalicz, P.; Zagyvai-Kiss, K.A.; Gribovszki, Z.; Bezak, N. Assessing the Impacting Factors Responsible for the Variation in the Throughfall Rate of Black Pine Trees in Diverse Urban Climates. In Proceedings of the EGU General Assembly 2025, Vienna, Austria, 27 April–2 May 2025; p. EGU25-4363. [CrossRef]
28. Gribovszki, Z.; Kalicz, P.; Palocz-Andresen, M.; Szalay, D.; Varga, T. Hydrological Role of Central European Forests in Changing Climate—Review. *Idojaras* **2019**, *123*, 535–550. [CrossRef]
29. Chunilal, K.A. A Review on Infiltration Patterns in Different Types of Soils. *Int. J. Res. Appl. Sci. Eng. Technol.* **2025**, *13*, 1267–1274. [CrossRef]
30. Allen, S.T.; Keim, R.F.; McDonnell, J.J. Spatial Patterns of Throughfall Isotopic Composition at the Event and Seasonal Timescales. *J. Hydrol.* **2015**, *522*, 58–66. [CrossRef]
31. Xu, X.; Guan, H.D.; Deng, Z.J. Isotopic Composition of Throughfall in Pine Plantation and Native Eucalyptus Forest in South Australia. *J. Hydrol.* **2014**, *514*, 150–157. [CrossRef]
32. Pinos, J.; Latron, J.; Nanko, K.; Levia, D.F.; Llorens, P. Throughfall Isotopic Composition in Relation to Drop Size at the Intra-Event Scale in a Mediterranean Scots Pine Stand. *Hydrol. Earth Syst. Sci.* **2020**, *24*, 4675–4690. [CrossRef]
33. Stockinger, M.P.; Lücke, A.; Vereecken, H.; Bogena, H.R. Accounting for Seasonal Isotopic Patterns of Forest Canopy Intercepted Precipitation in Streamflow Modeling. *J. Hydrol.* **2017**, *555*, 31–40. [CrossRef]
34. Vreča, P.; Pavšek, A.; Kocman, D. SLONIP—A Slovenian Web-Based Interactive Research Platform on Water Isotopes in Precipitation. *Water* **2022**, *14*, 2127. [CrossRef]
35. Vreča, P.; Malenšek, N. Slovenian Network of Isotopes in Precipitation (SLONIP)—A Review of Activities in the Period 1981–2015. *Geologija* **2016**, *59*, 67–83. [CrossRef]
36. Popp, A.L.; Beria, H.; Sprenger, M.; Ala-Aho, P.; Coenders-Gerrits, M.; Groh, J.; Klaus, J.; Knapp, J.L.A.; Koren, G.; Bakiri, I.; et al. Recent Advances in Tracer-Aided Mixing Modeling of Water in the Critical Zone. *Rev. Geophys.* **2025**, *63*, e2024RG000866. [CrossRef]
37. Sprenger, M.; Allen, S.T. What Ecohydrologic Separation Is and Where We Can Go with It. *Water Resour. Res.* **2020**, *56*, e2020WR027238. [CrossRef]
38. Brooks, J.R.; Barnard, H.R.; Coulombe, R.; McDonnell, J.J. Ecohydrologic Separation of Water between Trees and Streams in a Mediterranean Climate. *Nat. Geosci.* **2010**, *3*, 100–104. [CrossRef]
39. GURS Digital Elevation Model 2017. Available online: https://ipi.eprostor.gov.si/jgp/data (accessed on 22 December 2025).
40. Gačnik, J.; Žagar, K.; Hatvani, I.G.; Kern, Z.; Vreča, P. Climate Change Reflected in 40-Year Isotopic Composition Trends of Precipitation in Slovenia. *Environ. Res.* **2026**, *288*, 123286. [CrossRef]
41. Slovenian Environmental Agency. Klimatološka Povprečja (1981–2010). 2025. Available online: https://meteo.arso.gov.si/met/sl/climate/tables/normals_81_10/ (accessed on 23 December 2025).
42. Meteo. Si-ARHIV-Opazovani in Merjeni Meteorološki Podatki Po Sloveniji. Available online: https://meteo.arso.gov.si/met/sl/archive/ (accessed on 22 December 2025).
43. Koren Pepelnik, K.; Rman, N.; Žagar, K.; Vreča, P. Isotopic Characterisation of Precipitation and Throughfall Across Forest, Rural, and Urban Environments in Slovenia, During 2022–2024 Sampling Campaign. 2025. Available online: https://zenodo.org/records/17723128 (accessed on 19 March 2026).
44. Koren Pepelnik, K.; Rman, N.; Žagar, K.; Vreča, P. Comparability of Precipitation Isotopic Patterns Across Forest, Rural, and Urban Environments. *Acta Geogr. Slov.* **2026**. *submitted*.
45. Vreča, P.; Kanduč, T.; Štrok, M.; Žagar, K.; Nigro, M.; Barsanti, M. An Assessment of Six Years of Precipitation Stable Isotope and Tritium Activity Concentration Records at Station Sv. Urban, Eastern Slovenia. *Water* **2024**, *16*, 469. [CrossRef]

46. Picarro, Inc. L2130-i Analyzer Datasheet | Picarro. Available online: https://www.picarro.com/sites/default/files/product_documents/Picarro_L2130-i%20Analyzer%20Datasheet_250908.pdf (accessed on 8 March 2026).
47. Epstein, S.; Mayeda, T. Variation of O18 Content of Waters from Natural Sources. *Geochim. Cosmochim. Acta* **1953**, *4*, 213–224. [CrossRef]
48. Coplen, T.B.; Wildman, J.D.; Chen, J. Improvements in the Gaseous Hydrogen-Water Equilibration Technique for Hydrogen Isotope-Ratio Analysis. *Anal. Chem.* **1991**, *63*, 910–912. [CrossRef]
49. Avak, H.; Brand, W.A. The Finning MAT HDO-Equilibration-A Fully Automated H2O/Gas Phase Equilibration System for Hydrogen and Oxygen Isotope Analyses. *Thermo Electron. Corp. Appl. News* **1995**, *11*, 1–13.
50. Lancaster, S.T.; Irrgeher, J.; Dallmayr, R.; Conrad, E.; Hörhold, M.; Bohleber, P.; Behrens, M.; Camin, F.; Žagar, K.; Vreča, P.; et al. δ(18O/16O) Determinations in Water Using Inductively Coupled Plasma–Tandem Mass Spectrometry. *Anal. Chem.* **2025**, *97*, 20788–20797. [CrossRef]
51. Coplen, T.B. Reporting of Stable Hydrogen, Carbon, and Oxygen Isotopic Abundances. *Geothermics* **1995**, *24*, 707–712. [CrossRef]
52. Dansgaard, W. Stable Isotopes in Precipitation. *Tellus* **1964**, *16*, 436–468. [CrossRef]
53. Natali, S.; Doveri, M.; Giannecchini, R.; Baneschi, I.; Zanchetta, G. Is the Deuterium Excess in Precipitation a Reliable Tracer of Moisture Sources and Water Resources Fate in the Western Mediterranean? New Insights from Apuan Alps (Italy). *J. Hydrol.* **2022**, *614*, 128497. [CrossRef]
54. Masiol, M.; Zannoni, D.; Stenni, B.; Dreossi, G.; Zini, L.; Calligaris, C.; Karlicek, D.; Michelini, M.; Flora, O.; Cucchi, F.; et al. Spatial Distribution and Interannual Trends of δ18O, δ2H, and Deuterium Excess in Precipitation across North-Eastern Italy. *J. Hydrol.* **2021**, *598*, 125749. [CrossRef]
55. Juhlke, T.R.; Meier, C.; Geldern, R.V.; Vanselow, K.A.; Wernicke, J.; Baidulloeva, J.; Barth, J.A.C.; Weise, S.M. Assessing Moisture Sources of Precipitation in the Western Pamir Mountains (Tajikistan, Central Asia) Using Deuterium Excess. *Tellus B Chem. Phys. Meteorol.* **2019**, *71*, 1601987. [CrossRef]
56. Natali, S.; Baneschi, I.; Doveri, M.; Giannecchini, R.; Selmo, E.; Zanchetta, G. Meteorological and Geographical Control on Stable Isotopic Signature of Precipitation in a Western Mediterranean Area (Tuscany, Italy): Disentangling a Complex Signal. *J. Hydrol.* **2021**, *603*, 126944. [CrossRef]
57. Vertačnik, G.; Bertalanič, R.; Draksler, A.; Dolinar, M.; Vlahović, Ž.; Frantar, P. Podnebna Spremenljivost Slovenije v Obdobju 1961–2011; Ljubljana. 2018. Available online: https://meteo.arso.gov.si/uploads/probase/www/climate/text/sl/publications/PSSbrosura_spread_SLO.pdf (accessed on 25 December 2025).
58. Scherrer, S.C.; de Valk, C.; Begert, M.; Gubler, S.; Kotlarski, S.; Croci-Maspoli, M. Estimating Trends and the Current Climate Mean in a Changing Climate. *Clim. Serv.* **2024**, *33*, 100428. [CrossRef]
59. Ockerman, D.H.; Goldsman, D. Theory and Methodology Student T-Tests and Compound Tests to Detect Transients in Simulated Time Series. *Eur. J. Oper. Res.* **1999**, *116*, 681–691. [CrossRef]
60. Hawkins, E.; Williams, R.G.; Young, P.J.; Berardelli, J.; Burgess, S.N.; Highwood, E.; Randel, W.; Roussenov, V.; Smith, D.; Placky, B.W. Warming Stripes Spark Climate Conversations: From the Ocean to the Stratosphere. *Bull. Am. Meteorol. Soc.* **2025**, *106*, E964–E970. [CrossRef]
61. Copernicus European (EDO) and Global (GDO) Drought Observatories. *Standardized Precipitation Index (SPI)*; European Union: Brussels, Belgium, 2025. Available online: https://drought.emergency.copernicus.eu/data/factsheets/factsheet_spi.pdf (accessed on 23 December 2025).
62. Posit Team. *RStudio: Integrated Development Environment for R*; Posit Software, PBC: Boston, MA, USA, 2025. Available online: http://www.posit.co/ (accessed on 23 December 2025).
63. Craig, H. Isotopic Variations in Meteoric Waters. *Science* **1961**, *133*, 1702–1703. [CrossRef] [PubMed]
64. Kendall, K.A.; Shanley, J.B.; McDonnell, J.J. A Hydrometric and Geochemical Approach to Test the Transmissivity Feedback Hypothesis during Snowmelt. *J. Hydrol.* **1999**, *219*, 188–205. [CrossRef]
65. Gat, J.R. The Isotopic Composition of Evaporating Waters–Review of the Historical Evolution Leading up to the Craig–Gordon Model. *Isot. Environ. Health Stud.* **2008**, *44*, 5–9. [CrossRef]
66. Arosio, T.; Büntgen, U.; Nicolussi, K.; Moseley, G.E.; Saurer, M.; Pichler, T.; Smith, M.P.; Gutierrez, E.; Andreu-Hayles, L.; Hajdas, I.; et al. Tree-Ring δ18O and δ2H Stable Isotopes Reflect the Global Meteoric Water Line. *Front. Earth Sci.* **2024**, *12*, 1440064. [CrossRef]
67. Hatvani, I.G.; Smati, A.E.; Erdélyi, D.; Szatmári, G.; Vreča, P.; Kern, Z. Modeling the Spatial Distribution of the Meteoric Water Line of Modern Precipitation across the Broader Mediterranean Region. *J. Hydrol.* **2023**, *617*, 128925. [CrossRef]
68. Durowoju, O.S.; Odiyo, J.O.; Ekosse, G.-I.E. Determination of Isotopic Composition of Rainwater to Generate Local Meteoric Water Line in Thohoyandou, Limpopo Province, South Africa. *Water SA* **2019**, *45*, 183–189. [CrossRef]
69. Benjamin, L.; Knobel, L.; Hall, L.; Cecil, L.; Green, J. *Development of a Local Meteoric Water Line for Southeastern Idaho, Western Wyoming, and South-Central Montana*; Scientific Investigations Report; United States Geological Survey: Reston, VA, USA, 2005.

70. Yurtsever, Y.; Araguas, L.A. Environmental Isotope Applications in Hydrology: An Overview of the IAEA's Activities, Experiences, and Prospects. In *Tracers in Hydrology*; International Association of Hydrological Sciences: Oxford, UK, 1993; pp. 3–20.
71. Putman, A.L.; Fiorella, R.P.; Bowen, G.J.; Cai, Z. A Global Perspective on Local Meteoric Water Lines: Meta-Analytic Insight into Fundamental Controls and Practical Constraints. *Water Res.* **2019**, *55*, 6896–6910. [CrossRef]
72. IAEA. *Statistical Treatment of Data on Environmental Isotopes in Precipitation*; IAEA: Vienna, Austria, 1992.
73. Carroll, R.J.; Ruppert, D. The Use and Misuse of Orthogonal Regression in Linear Errors-in-Variables Models. *Am. Stat.* **1996**, *50*, 1–6. [CrossRef]
74. Crawford, J.; Hughes, C.E.; Lykoudis, S. Alternative Least Squares Methods for Determining the Meteoric Water Line, Demonstrated Using GNIP Data. *J. Hydrol.* **2014**, *519*, 2331–2340. [CrossRef]
75. Hughes, C.E.; Crawford, J. A New Precipitation Weighted Method for Determining the Meteoric Water Line for Hydrological Applications Demonstrated Using Australian and Global GNIP Data. *J. Hydrol.* **2012**, *464–465*, 344–351. [CrossRef]
76. Vachon, R.W.; Welker, J.M.; White, J.W.C.; Vaughn, B.H. Monthly Precipitation Isoscapes (δ18O) of the United States: Connections with Surface Temperatures, Moisture Source Conditions, and Air Mass Trajectories. *J. Geophys. Res. Atmos.* **2010**, *115*, D21. [CrossRef]
77. Rozanski, K.; Araguás-Araguás, L.; Gonfiantini, R. Isotopic Patterns in Modern Global Precipitation. *Geophys. Monogr. Ser.* **1993**, *78*, 1–36. [CrossRef]
78. Zhang, J.; Chen, H.S.; Nie, Y.P.; Fu, Z.Y.; Lian, J.J.; Luo, Z.D.; Wang, F. Temporal Variations of Precipitation Driven by Local Meteorological Parameters in Southwest China: Insights from 9 Years of Continuous Hydro-Meteorological and Isotope Observations. *J. Hydrol.-Reg. Stud.* **2023**, *46*, 101345. [CrossRef]
79. Allen, S.T.; Jasechko, S.; Berghuijs, W.R.; Welker, J.M.; Goldsmith, G.R.; Kirchner, J.W. Global Sinusoidal Seasonality in Precipitation Isotopes. *Hydrol. Earth Syst. Sci.* **2019**, *23*, 3423–3436. [CrossRef]
80. Kern, Z.; Hatvani, I. Technical Note: Mind the Gap–Benchmarking of Various Imputation Approaches for Precipitation Stable Isotope Time Series. *Egusphere* **2025**, *preprint*. [CrossRef]
81. Burgman, J.O.; Calles, B.; Westman, F. Conclusions from a Ten Year Study of Oxygen-18 in Precipitation and Runoff in Sweden. In *Isotope Techniques in Water Resources Development*; IAEA: Vienna, Austria, 1987; pp. 579–590.
82. Niinikoski, P.I.; Hendriksson, N.M.; Karhu, J.A. Using Stable Isotopes to Resolve Transit Times and Travel Routes of River Water: A Case Study from Southern Finland. *Isot. Environ. Health Stud.* **2016**, *52*, 380–392. [CrossRef]
83. Žagar, K.; Ortega, L.; Pavlič, U.; Jamnik, B.; Bračič Železnik, B.; Vreča, P. Unravelling the Sources Contributing to the Urban Water Supply: An Isotope Perspective from Ljubljana, Slovenia. *J. Hydrol.* **2024**, *632*, 130892. [CrossRef]
84. Koren Pepelnik, K.; Rman, N.; Žagar, K.; Vreča, P. The role of isotopes in precipitation in assessing the impact of climate change on forest mortality. In Proceedings of the EMS Annual Meeting 2025, Ljubljana, Slovenia, 7–12 September 2025; p. EMS2025-469. [CrossRef]
85. Kobold, M. *Hidrološka Suša Površinskih Voda v Letu 2022 in Primerjava s Sušnimi Leti 1993, 2003 in 2012*; ARSO: Ljubljana, Slovenia, 2022. Available online: https://hmljn.arso.gov.si/vode/poro%C4%8Dila%20in%20publikacije/Hidrolo%C5%A1ka%20su%C5%A1a%20povr%C5%A1inskih%20voda%202022.pdf (accessed on 19 March 2026).
86. Vreča, P.; Bronić, I.K.; Leis, A.; Demšar, M. Isotopic Composition of Precipitation at the Station Ljubljana (Reaktor), Slovenia-Period 2007–2010. *Geologija* **2014**, *57*, 217–230. [CrossRef]
87. Vreča, P.; Bronić, I.K.; Horvatinčić, N.; Barešić, J. Isotopic Characteristics of Precipitation in Slovenia and Croatia: Comparison of Continental and Maritime Stations. *J. Hydrol.* **2006**, *330*, 457–469. [CrossRef]
88. Vreča, P.; Bronić, I.K.; Leis, A.; Brenčič, M. Isotopic Composition of Precipitation in Ljubljana (Slovenia). *Geologija* **2008**, *51*, 169–180. [CrossRef]
89. Bronić, I.K.; Barešić, J.; Borković, D.; Sironić, A.; Mikelić, I.L.; Vreča, P. Long-Term Isotope Records of Precipitation in Zagreb, Croatia. *Water* **2020**, *12*, 226. [CrossRef]
90. Froehlich, K.; Gibson, J.J.; Aggarwal, P.K. Deuterium Excess in Precipitation and Its Climatological Significance. In *Proceedings of the Study of Environmental Change Using Isotope Techniques*; International Atomic Energy Agency (IAEA): Vienna, Austria, 2002; pp. 54–66. Available online: https://inis.iaea.org/records/50trx-hjw91 (accessed on 25 December 2025).
91. Krklec, K.; Domínguez-Villar, D.; Lojen, S. The Impact of Moisture Sources on the Oxygen Isotope Composition of Precipitation at a Continental Site in Central Europe. *J. Hydrol.* **2018**, *561*, 810–821. [CrossRef]
92. Ciric, D.; Nieto, R.; Losada, L.; Drumond, A.; Gimeno, L. The Mediterranean Moisture Contribution to Climatological and Extreme Monthly Continental Precipitation. *Water* **2018**, *10*, 519. [CrossRef]
93. Gomez-Sanz, V.; Garcia-Viñas, J.I. Soil Moisture Spatio-Temporal Behavior of Pinus Pinaster Stands on Sandy Flatlands of Central Spain. *For. Syst.* **2011**, *20*, 293–302. [CrossRef]
94. Tao, S.; Xu, J.; Xia, J.; Xiao, Y. Influence of sub-cloud evaporation on precipitation isotopes: Insights from hourly-scale meteorological assessment in a large lake in the East Asian monsoon region. *Hydrol. Process.* **2025**, *39*, e70152. [CrossRef]

95. Deuterium Excess in Precipitation Reveals Water Vapor Source in the Monsoon Margin Sites in Northwest China. Available online: https://www.mdpi.com/2073-4441/12/12/3315 (accessed on 23 December 2025).
96. Vreča, P.; Brenčič, M.; Leis, A. Comparison of Monthly and Daily Isotopic Composition of Precipitation in the Coastal Area of Slovenia. *Isot. Environ. Health Stud.* **2007**, *43*, 307–321. [CrossRef] [PubMed]
97. Liotta, M.; Favara, R.; Valenza, M. Isotopic Composition of the Precipitations in the Central Mediterranean: Origin Marks and Orographic Precipitation Effects. *J. Geophys. Res. Atmos.* **2006**, *111*, D19. [CrossRef]
98. Fritz, M.; Wetterich, S.; McAlister, J.; Meyer, H. A New Local Meteoric Water Line for Inuvik (NT, Canada). *Earth Syst. Sci. Data* **2022**, *14*, 57–63. [CrossRef]
99. Lee, J.-E.; Fung, I. "Amount Effect" of Water Isotopes and Quantitative Analysis of Post-Condensation Processes. *Hydrol. Process.* **2008**, *22*, 1–8. [CrossRef]
100. Koren Pepelnik, K.; Janža, M.; Čater, M.; Čenčur Curk, B. Ecohydrological Methods for Characterizing Groundwater Dependence of Terrestrial Ecosystems to Support Sustainable Water Resources Management: A Review. *Ecotoxicol. Environ. Saf.* **2026**. *submitted*.
101. European Communities. Water Framework Directive (2000/60/EC). In *Technical Report on Groundwater Dependent Terrestrial Ecosystems*; European Communities: Brussels, Belgium, 2011.
102. Baaner, L.; Anker, H.T.; Ejrnæs, R. The Water Framework Directive's Protection of Groundwater-Dependent Terrestrial Ecosystems. *Ambio* **2025**, *54*, 808–817. [CrossRef] [PubMed]